Proceedings of NUMIFORM 2019: The 13th International Conference on Numerical Methods in Industrial Forming Processes
Editors: Yannis Korkolis, Brad Kinsey, Marko Knezevic, and Nikhil Padhye

EFFECT OF MATRIX VISCOELASTICITY ON PREDICTION OF RESIDUAL STRESSES IN ORTHOGONAL 3D WOVEN COMPOSITES

H. Galdino da Silva[1], B. Drach[1*], K. Vasylevskyi[2], I. Tsukrov[2], T. Gross[2]

[1]Mechanical & Aerospace Engineering, New Mexico State University, 1040 S. Horseshoe St., Jett Hall, Room 104, Las Cruces, NM, 88003, USA

[2]Mechanical Engineering, University of New Hampshire, Kingsbury Hall, W101, 33 Academic Way, Durham, NH, 03824, USA

*Corresponding Author, (borys@nmsu.edu)

Keywords: residual stress, viscoelasticity, finite element analysis, 3D woven composites, curing

Abstract

In this paper, the effect of matrix viscoelasticity on the development of residual stresses in 3D woven composites is investigated using Finite Element Analysis. Based on experimental observations, it is hypothesized, that the stresses develop mainly due to the difference in the coefficients of thermal expansion between the fiber reinforcement and the matrix. The model considered is a “1x1 orthogonal” 3D woven composite unit cell that is generated using x-ray computed microtomography data. In this study, cooling after curing is considered under the assumption of zero stress at the beginning of the cooling. In addition to the full time- and temperature-dependent viscoelastic formulation, the applicability of two simplified constitutive methods, elastic and variable time pseudo-viscoelastic, is investigated. It is observed that the pseudo-viscoelastic method predicts similar cumulative stress distribution (Von Mises and Hydrostatic) compared to the full viscoelastic results. The elastic model presented the highest stress values while the full viscoelastic model presented the lowest stress values.

1. Introduction

3D woven composite materials have increasingly been used in the aerospace industry due to their high delamination and impact resistance compared to the traditional laminated composites [1, 2]. Based on the experimental observations [3], it is hypothesized that two major factors are responsible for high residual stresses contributing to microcracking of 3D woven composites: the large difference in the coefficient of thermal expansion (CTEs) between the fiber reinforcement and the matrix and the large amount of through-thickness reinforcement [4, 5]. Accurate numerical prediction of the residual stresses depends on the fidelity of geometric modeling and constitutive material models. In particular, time- and temperature-dependent viscoelasticity of the matrix must be included because it may result in significant stress relaxation in the composites [6 - 8]. At the same time, the full viscoelastic formulation requires extensive material characterization and computational resources. It has been shown that “simple” constitutive models [9] can be used to predict residual stresses and dimensional stability in asymmetric composite plates with reasonable accuracy. Other methods have been studied under different curing cycles and validated using experimental results [1].

In this paper, the residual stresses in a "1x1 orthogonal" 3D woven carbon/epoxy composite is analyzed using Finite Element Analysis (FEA). A single periodic unit cell of the reinforcement architecture shown in Figure 1 was obtained from microtomography data. In this analysis, it is assumed that the tows have time- and temperature-independent material properties [5] due to low matrix volume fraction in the tows (approximately 20%). The thermoset viscoelastic matrix surrounding the tows is modeled using three different constitutive models: full viscoelastic (implemented via Prony series); variable time pseudo-viscoelastic; and elastic. The three models are compared based on the cumulative volume residual stress distribution (Von Mises and Hydrostatic) and simulation time. The full viscoelastic model is assumed as the most realistic prediction of stresses, and the pseudo-viscoelastic predictions and the elastic predictions are compared to the full viscoelastic model.

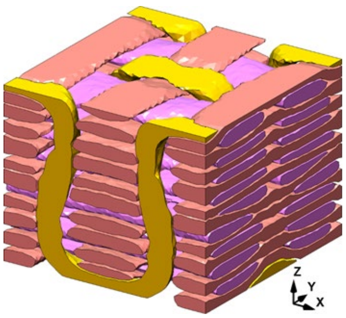

Figure 1. "1x1 orthogonal" woven composite: realistic geometry

2. Modeling Approach

Three constitutive models are considered: viscoelastic, pseudo-viscoelastic, and elastic.

2.1. Viscoelastic Model

The isotropic material properties of the matrix depend on both time and temperature in this case. The Young's modulus (E) was extracted from experimental data [10] and the shear modulus (G) and bulk modulus (K) were derived assuming the constant Poisson's ratio $\nu = 0.35$. Prony series was fitted to the data using the commercial FEA software package MSC Marc Mentat. The relaxation function used G as follows (similar function was used for K):

$$G(t,T) = G^{(\infty)} + \sum_{k=1}^{N} G^{(k)} e^{\frac{-ta(T)}{\tau_k}}$$

where t is time (s), T is temperature (℃), τ_k is relaxation time (s), N is the order of the series, $a(T)$ is the Thermo-Rheologically Simple shift function (Williams-Landel-Ferry shift function with coefficients $c_1 = 1790.35$, $c_2 = 14028.2$, and reference temperature $T_{ref} = 100℃$ is used), $G^{(\infty)}$ is the long-term stiffness, and $G^{(k)}$ is the fitting parameter. From the short-term ($t = 0$) moduli G and K, the short-term E and ν are found as $4.875\ \mathrm{GPa}$ and 0.3589, respectively.

2.2. Variable Time Pseudo-Viscoelastic Model

In this model, the Young's modulus is a function of temperature only; however, values of E are extracted from the relaxation curves [10] at different time instants (as opposed to $t = 0$), hence the values of E (Figure 2) take into account some relaxation and are easily implemented. The resulting behavior is path independent and, therefore, the simulation can be performed in a single step.

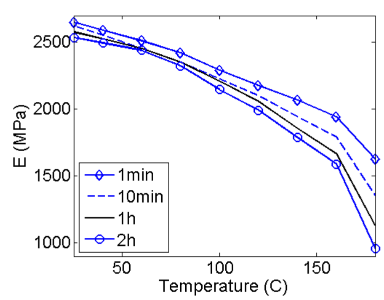

Figure 2. Young's Modulus vs Temperature

2.3. Elastic Model

Isotropic material properties are dependent only on temperature. The matrix Young's modulus and CTE are linear functions of temperature: $E_{0°C} = 3.5\,\text{GPa}$ and $E_{180°C} = 2.438\,\text{GPa}$; $\text{CTE}_{0°C} = 5 \cdot 10^{-5}\,°\text{C}^{-1}$ and $\text{CTE}_{180°C} = 6.89 \cdot 10^{-5}\,°\text{C}^{-1}$; $\nu = 0.35$. In this case, time-dependent relaxation does not occur and numerical simulations can be carried out in a single step.

2.4. Boundary and Initial Conditions

Periodic boundary conditions (PBCs) in the X and Y directions are applied to simulate the response of a large composite panel by considering a single unit cell. In the current implementation, contraction of the unit cell due to the temperature drop is permitted, but the node displacements on the opposite faces of the cell are kept periodic. The PBCs are based on [11] without constraining the through-thickness direction (Z-axis). All models are subjected to the same linear temperature decrease from the curing temperature $T_0 = 165\,°C$ (applied as the initial condition) to the room temperature $T_{1700s} = 25\,°C$ over 1700 seconds assuming zero initial stress. The temperature change is assumed to happen in all elements simultaneously due to the relatively slow cooling rate, see [5].

3. Results

The results are presented in Figure 3 and Table I. The cumulative stress distributions presented in Figure 3b and Figure 3c show fractions of the overall matrix volume with stresses below a given Von Mises or hydrostatic stress value. The plots indicate that both considered approximations overestimate residual stresses (compared to the full viscoelastic formulation) – the full viscoelastic model results are at the far left side of the plot (low stress values), the elastic results are at the far right side (high stress values), and the pseudo-viscoelastic values fall between the two. The pseudo-viscoelastic curve "2 hours" (i.e. Young's moduli values sampled from the material relaxation curves at $t = 2\,h$) indicates that stresses in the matrix material are more relaxed compared to the curves "1min", "10 min" and "1 hour" and is close to the viscoelastic stress distribution. However, the difference among the four pseudo-viscoelastic curves is small.

Table I. Comparison of the predicted stress percentiles (99, 95 and 50) obtained from the pseudo-viscoelastic (2 hours) and elastic models with the full viscoelastic results

	Percentile	Viscoelastic model	Pseudo-Viscoelastic model	% difference	Elastic	% difference
Von Mises (MPa)	99	49.5	53.6	8.4	66.9	35.2
	95	33.6	36.6	9.1	47.3	40.8
	50	23.3	25.8	10.6	34.2	46.7
Hydrostatic (MPa)	99	42.8	47.6	11.1	61.7	44.2
	95	29.1	32.5	11.8	43.6	50.1
	50	20.2	22.8	13.3	31.5	56.4
Runtime (h)	-	18.5	0.16	-	0.16	-

4. Conclusions

In this paper, three constitutive models have been investigated. Using the full temperature- and time-dependent viscoelastic model results as the "correct" stress distribution, the "2 hours" pseudo-viscoelastic method resulted in a much smaller difference than the elastic method – the maximum difference of 13.3% vs. the maximum difference of 56.4%, correspondingly. Given the relatively small difference in the stress values and the 100x times faster simulation runtime, the pseudo-viscoelastic method is an efficient way of estimating residual stresses compared to the full viscoelastic formulation.

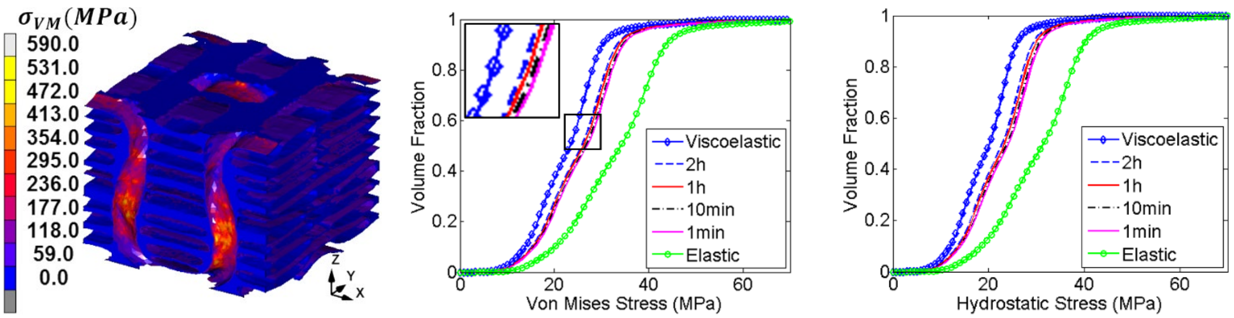

(a) (b) (c)

Figure 3. FEA Results: (a) Von Mises stress distribution in the matrix (full viscoelastic model); (b) cumulative volume Von Mises stress distribution; (c) cumulative volume hydrostatic stress distribution.

5. Acknowledgements

This material is based upon work supported by the National Science Foundation under Grant No. CMMI-1662098. We are grateful to Adam Ewert for his help with geometric modeling and FEA model preparation for the orthogonal architecture.

6. References

[1] N. Zobeiry *et al.*, “Multiscale characterization and representation of composite materials during processing,” *Phil. Trans. R. Soc. A*, vol. 374:201502, no. 2071, 2016.

[2] L. E. Asp, E. Marklund, J. Varna, and R. Olsson, “Multiscale Modelling of Non-Crimp Fabric Composites,” *Proc. 2012 Int. Mech. Eng. Congr. Expo.*, pp. 1–10, 2012.

[3] M. Gigliotti, Y. Pannier, R. A. Gonzalez, M. C. Lafarie-Frenot, and S. V. Lomov, “X-ray micro-computed-tomography characterization of cracks induced by thermal cycling in non-crimp 3D orthogonal woven composite materials with porosity,” *Compos. Part A Appl. Sci. Manuf.*, vol. 112, pp. 100–110, 2018.

[4] I. Tsukrov, B. Drach, H. Bayraktar, and J. Goering, “Modeling of Cure-Induced Residual Stresses in 3D Woven Composites of Different Reinforcement Architectures,” *Key Eng. Mater.*, vol. 577–578, pp. 253–256, 2013.

[5] I. Tsukrov, K. Vasylevskyi, B. Drach, H. Buntrock, and T. Gross, “Utilizing numerical models to identify process-induced residual stresses in 3D woven carbon/epoxy composites,” *IOP Conf. Ser. Mater. Sci. Eng.*, vol. 406, no. 1, 2018.

[6] M. Benavente, L. Marcin, A. Courtois, M. Lévesque, and E. Ruiz, “Numerical analysis of viscoelastic process-induced residual distortions during manufacturing and post-curing,” *Compos. Part A Appl. Sci. Manuf.*, vol. 107, pp. 205–216, 2018.

[7] M. Hirsekorn, L. Marcin, and T. Godon, “Multi-scale modeling of the viscoelastic behavior of 3D woven composites,” *Compos. Part A Appl. Sci. Manuf.*, vol. 112, no. May, pp. 539–548, 2018.

[8] Y. K. Kim and S. R. White, “Viscoelastic Analysis of Processing-Induced Residual Stresses in Thick Composite Laminates,” *Mech. Adv. Mater. Struct.*, vol. 4, no. 4, pp. 361–387, 1997.

[9] A. Ding, S. Li, J. Sun, J. Wang, and L. Zu, *A thermo-viscoelastic model of process-induced residual stresses in composite structures with considering thermal dependence*, vol. 136. Elsevier Ltd, 2016.

[10] C. Brauner, T. B. Block, H. Purol, and A. S. Herrmann, “Microlevel manufacturing process simulation of carbon fiber/epoxy composites to analyze the effect of chemical and thermal induced residual stresses,” *J. Compos. Mater.*, vol. 46, no. 17, pp. 2123–2143, 2012.

[11] B. Drach, I. Tsukrov, and A. Trofimov, “Comparison of full field and single pore approaches to homogenization of linearly elastic materials with pores of regular and irregular shapes,” *Int. J. Solids Struct.*, vol. 96, pp. 48–63, 2016.